Modeling Liquid Phase Sintering of Hard metal powder compacts

Shama Shamasundar *, Mahesha Siddegowda* , Pavanachand Chigurupati , Rengarajan Raghavan***, Ramesh Rao. S. *****

* ProSIM – AFTC
# 326, 8th Main, III Stage, IV Block, Basaveshwarnagar,
Bangalore -560 079, INDIA
e-mail : *info@pro-sim.com*

** Scientific Forming Technologies Corporation
5038 Reed Road, Columbus, Ohio, USA - 43220
e-mail : *pchigurupati@deform.com*

***Widia India Limited
8/9th mile, Tumkur Road.
Bangalore – 560073, INDIA
e-mail : *rr@widiaindia.com*

ABASTRACT

The yield function and the constitutive equations developed for hardmetal powders are incorporated into a non-linear FEM simulation engine. Densification due to particle rearrangement, melting of additive particles, contact flattening, pore size distribution & liquid pressure are modeled by choosing appropriate governing equations. Using the density gradients resulting from the compaction process, the differential shrinkage at different regions in the compact are predicted. The experimental measurements and model predicted results are compared. Details of model development, FE analysis and validation are discussed with reference to different compact shapes and grades of powder. It is demonstrated that FEM simulations can be employed as a tool in the design process, to minimize/eliminate undesirable shrinkage related distortion in liquid phase sintering of hardmetal compact.

1: INTRODUCTION

Liquid phase sintering is defined as "*The thermal treatment of powder compact at a temperature below the melting point of the main constituent, for the purpose of increasing its strength by bonding together of the particles*". In case of powder mixtures the sintering temperatures may be above the melting point of the low melting constituent and below the melting point of the base material e.g. tungsten carbide/cobalt, iron/copper, copper/tin, so that the sintering takes place in the presence of liquid phase which is formed by the melting of low melting material, hence the term "Liquid Phase Sintering".

The liquid phase accelerates the sintering process. Main advantages of liquid phase sintering are low sintering temperature, fast densification, homogenization, and high final densities. Mechanical and physical properties of liquid phase sintered parts are superior to solid-state sintered parts [1]. However shrinkage associated with the densification during sintering process poses major challenge for the designers. In case of liquid phase sintering of hardmetal compact the amount of linear shrinkage will be as

high as 17-22%. Industrial designers are concerned with the effect of distortion arising due to differential shrinkage in the component during sintering. Shrinkage during sintering is a function of local relative density in the green compact. Variation of density in the green compact arise as a result of friction between powder and die/tool wall, geometry, differential punch/die movement, material flow characteristics and so on.

Sintering behavior is studied by various researchers [1-8,10,11], have modeled basic phenomenology of sintering through mathematical modeling. However at the industry level the designers still go through traditional trial and error methods during process design cycle. The present work is aimed towards developing liquid phase sintering model, which can be implemented in a FEM code and used in the industry as a design tool. In the present paper, development of model for liquid phase sintering of hard metals, implementing these models in a Finite Element code DEFORM™2D, and validation of the model with plant data [15] are discussed.

2: LIQUID PHASE SINTERING MODEL

The driving force for densification during sintering is the reduction in interfacial energy between particles. An appreciable volume fraction of liquid in the compact during sintering, an appreciable degree of solubility of solid in the liquid and complete wetting of solid particles by liquid are the desirable conditions for complete densification during liquid phase sintering. Densification during liquid phase sintering is a result of several mechanisms. These mechanisms get activated at different time/temperature during sintering [3].

Model for liquid phase sintering was developed in Svoboda et al. [1] and a model for liquid phase sintering applied to Si_3N_4 and WC-Co was developed by P.E. McHugh and H.Riedel [2]. The Liquid phase sintering model chosen for implementation comprises the following aspects of liquid phase sintering

- Primary rearrangement of the solid particles when the liquid phase is formed
- Grain shape accommodation by contact flattening
- Filling of large pores and grain coarsening in the final stage of sintering

The rearrangement dominates in the initial stage after liquid formation, shape accommodation in the second, and filling of large pores and grain coarsening in the final stage of sintering [2].

Model is formulated in terms of state variables: Solid volume fraction-D_s (relative density of solid) which is the ratio of volume fraction of solid phase to the entire volume of the component, flattening strain (δ), grain radius (R), and liquid volume fraction (g). The liquid fraction (g) is assumed to be a function of the temperature only, which in turn is a function of time. Equation for solid density is

$$\dot{D}_s = \dot{D}_s^r + \dot{D}_s^m + \dot{D}_s^f \qquad (1)$$

where dot denotes the derivative with respect to time and the superscripts indicate the contribution by rearrangement (r), melting of additive particles (m), and contact flattening (f). In the following sections the evolution equations for state variables are derived.

2.1: Particle rearrangement

During sintering liquid phase is formed in the compact at areas, which constitute low melting particles. Capillary forces pull this liquid into particle necks and small pores. The resulting liquid flow may lead to residual pores at initial sites, which will be filled in the later stages of sintering [8,9]. The penetration of liquid leads to swelling of compact resulting from increased particle distance due to the additional liquid

introduced into the contact areas. However the particle movement leads to rearrangement thus resulting in densification. The capillary forces exerted on the solid particles by liquid and applied mechanical pressure leads to the rearrangement of solid particles.

Rearrangement requires the sliding of particles against one another with a liquid film between particles. Hence the densification rate of the solid particles by rearrangement should be depend on the viscosity of the liquid - η, liquid film thickness - δ_b, and the area of the particle contacts - $\prod c^2$ in the following way.

$$\dot{D}_s^r = \frac{bD_s\delta_b R\left(\sigma_s - \sigma_m\right)\left(D_1 - D_S\right)}{\eta c^2} \qquad if\ D_1 > D_S$$
$$= 0 \qquad if\ D_1 \le D_S \tag{2}$$

where R is the radius of the solid particles, D_1 corresponds to the density of the random dense sphere packing, D_1=0.63, σ_s is the sintering stress, σ_m is the mean stress acting on the material, which is equal to the negative of the applied mechanical pressure, c is contact radius, b is a dimensionless factor related to viscosity (η), taken as unity in computation. The liquid film thickness δ_b is adopted form literature [3] to be in the order of 1.5nm.

2.2: Melting of additive particles

During sintering heating up to sintering temperature, the low melting point particles will melt and liquid phase is formed. The immediate effect of melting is to reduce the solid density according to

$$\dot{D}_s^m = -\frac{\dot{g}D_s}{1-g} \tag{3}$$

where g is the liquid volume fraction and the dot denotes the derivative with respect to time. The disappearance of additive particles and partial solution of the base material in the melt opens the possibility for rearrangement of the solid particles, so that the total density increases.

2.3: Contact flattening

The densification rate of solid particles due to contact flattening is given by

$$\dot{D}_s^f = \frac{3\dot{\delta}D_s}{\left(1-\delta\right)} \tag{4}$$

Where δ is the flattening strain and $\dot{\delta}$ is the flattening strain rate. δ grows by solution/precipitation of the solid in to the liquid film and diffusion of the dissolved solid atoms out of the contact area in to the liquid collar to be deposited by on the particle surface outside the contact area [12-14]. This phenomenon is explained in detail by Riedel [2].

4: IMPLEMENTATION OF MODEL AS CONSTITUTIVE EQUATION FOR NON –LINEAR FEM CODE

The constants and co-efficient, used in these mathematical models are dependent on the physical, chemical properties of constituents in powder mixture. Corresponding to the powder characteristics such

as solubility, liquid wetting, pressure, process conditions such as temperature and time, these constants and co-efficient have different value. Various material and process parameters will have to be determined as applicable to these material systems and processes. Often, the individual variables cannot be determined at the operating conditions. These are determined by inverse solutions. The data are derived from experimental results and running the models for these experiments in an iterative manner. By matching the experimental and model (theoretical / numerical) results, the corresponding material variable/constants are determined. Once the required set of variables, constants and co-efficient are determined in this manner, they can be used confidently in the model.

In the present work these mathematical equations [1,2,3,4,5], which model the liquid phase sintering, are implemented as a subroutine for non-linear FEM code DEFORM™ [16]. During sintering there are two major phenomena taking place. Heat transfer within the component and densification resulting in shrinkage or deformation of original shape. The FEM software in which sintering simulation has to be carried out should have the capability to handle coupled analysis of transient heat transfer and deformation (shrinkage). The sintering model subroutine is linked with the main solving engine of DEFORM™, so that sintering equations are solved for each nodal point to determine the sintering process variables at each step of temperature change against time. Figure-1 shows the flow chart for sintering process.

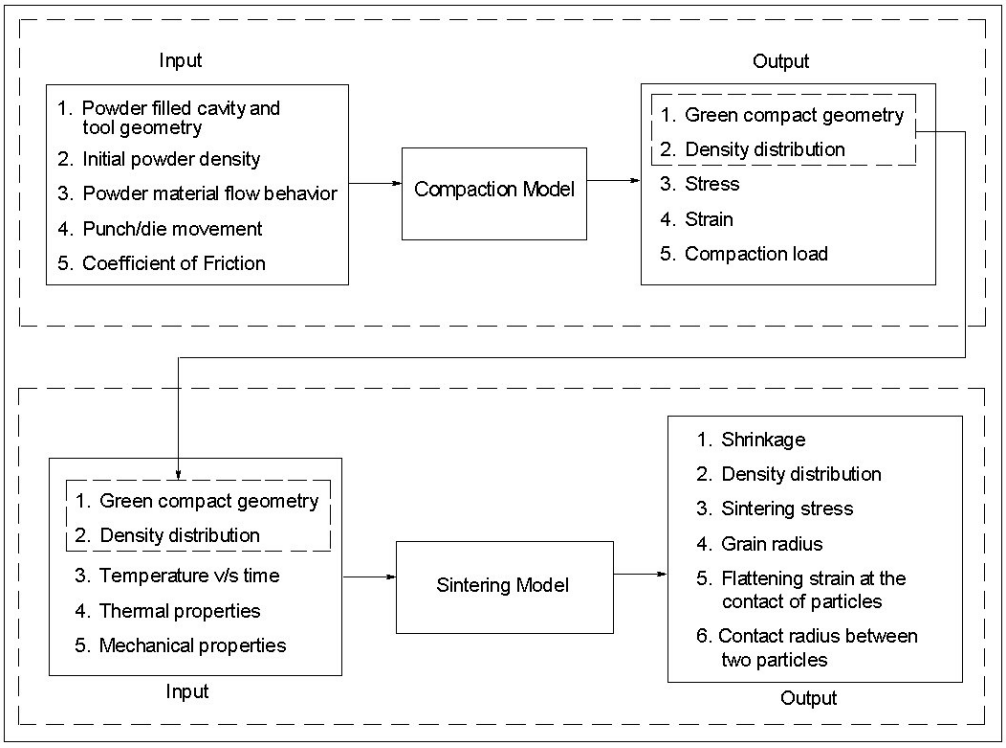

Figure 1. *Flow chart for powder compaction and sintering process modeling*

Input data is entered in to the model through DEFORM™ pre-processor. The FEM simulation engine does the calculation and in the DEFORM™ post-processor the output results are viewed both graphically and numerically. Density distribution in the green compact and compact geometry, which is the output of the powder compaction model, will go as an input in to the sintering model. Since shrinkage in liquid phase sintering is mainly dependent on density distribution in the green compact, to predict shrinkage and distortion accurately, it is important to determine the initial density distribution accurately. In the present work we have used DEFORM™ as a FEM code to simulate the powder compaction. The density

distribution predicted by DEFORM^{TM} is imported in to the sintering model and used as a input for modeling sintering behavior.

5: EXPERIMENTAL DETAILS

Validation of liquid phase sintering model was carried out for 15 experiments, which include three different component shapes and three different grades of powder. To simplify the validation and fine-tuning of the model, initial set of experiments were carried out with axis-symmetry components.

5.1: Component 1

First set of experiments were carried out choosing a cylindrical component. The powder filled cavity is a cylinder of 14mm diameter with a simple compaction procedure in which the pressing stroke is by downward movement of top punch with stationary die. Compacting to different heights will result in different average green density and different density gradients in the compact. Powder density at the end of die filling was measured to be 0.223 for grade-1, 0.218 for grade-2 and 0.245 for grade-3 powder. Figure 2a shows the density distribution after compaction (green density) and Figure 2b shows the component geometry after compaction (mesh with thin line) and after sintering (mesh with thick line) for the 16.20mm height green compact of grade-1 powder. Figure 2b shows only right half of the centrally cut section of the cylinder with central axis at the left hand side. With different compact height and powder material 12 different samples were obtained. The variation in density distribution after compaction has resulted in a taper in the vertical direction as shown in figure 2a. Hence diameter is measured at the top and bottom end of the component, where top end corresponds to top punch side and bottom corresponds to ejector side. Model prediction also capture the taper in the component.

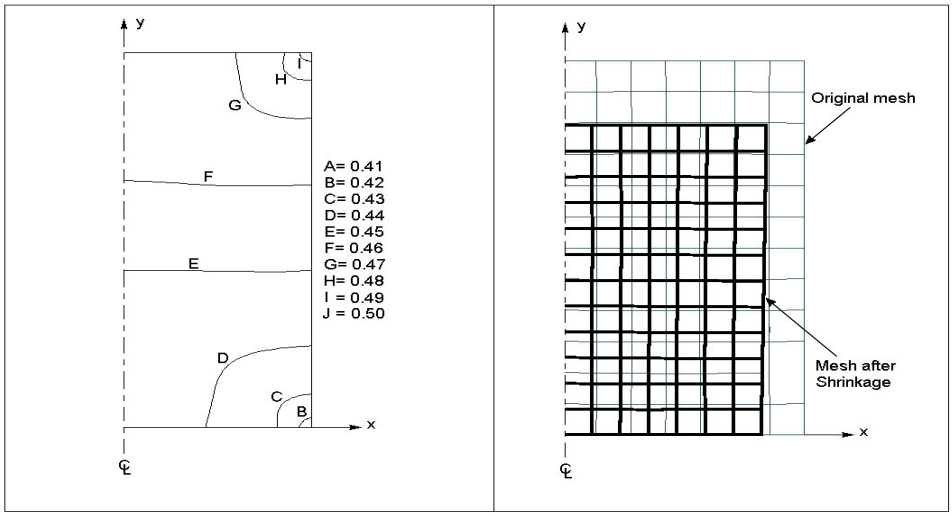

(a) (b)

Figure 2. (a). *Density distribution after compaction (b). The mesh before and after sintering*

* Details of compaction procedure and FEM modeling of compaction are given in an adjoining paper by the authors

Figure 3a shows the comparison between experimentally measured dimensions and model prediction for bottom diameter for grade-1 powder. The x-axis represents the average density and y-axis represents the bottom diameter. Experiments were conducted for 5 samples with different height resulting in nominal density or average density of 0.46, 0.48, 0.51, 0.54 and 0.57. Similarly experimentally measured top diameter and height of the component are compared with model predictions in figure 3b and 3c.

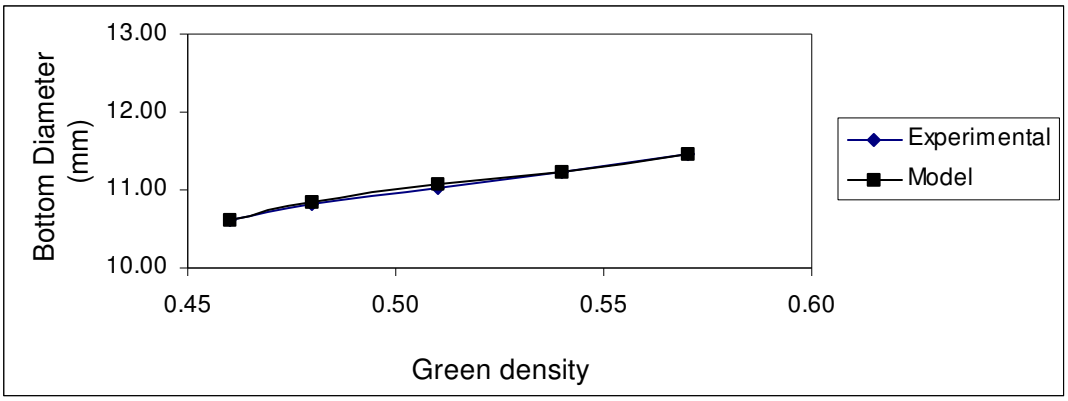

Figure 3 (a)

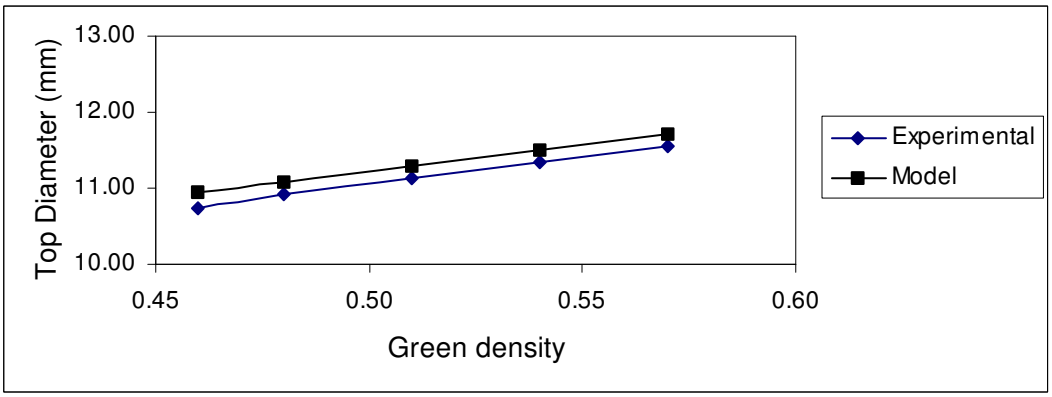

Figure 3 (b)

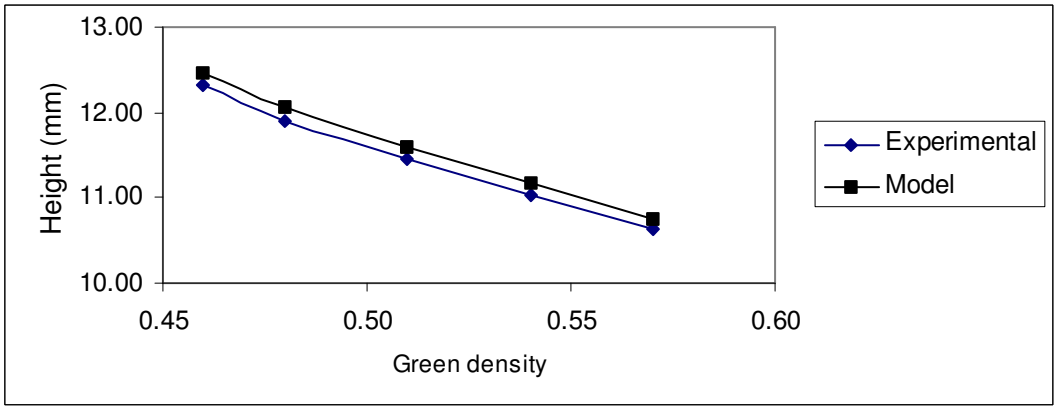

Figure 3 (c)

Figure 3. *Comparison of experimental results with model prediction for grade-1 powder material (a). bottom diameter (b). top diameter (c). height*

Experiments were conducted for the cylindrical component with grade-2 powder material, which has considerable difference from grade-1 with respect to composition, grain size and powder density (Appendix, Table-3). For this grade of material three samples were compacted for different heights and sintered. Average densities of these samples are 0.52, 0.53 and 0.56. Comparison of model prediction with experimental results for grade-2 shows similar trends as that of grade-1 powder material. The validation results are shown in figure 4a,b and c.

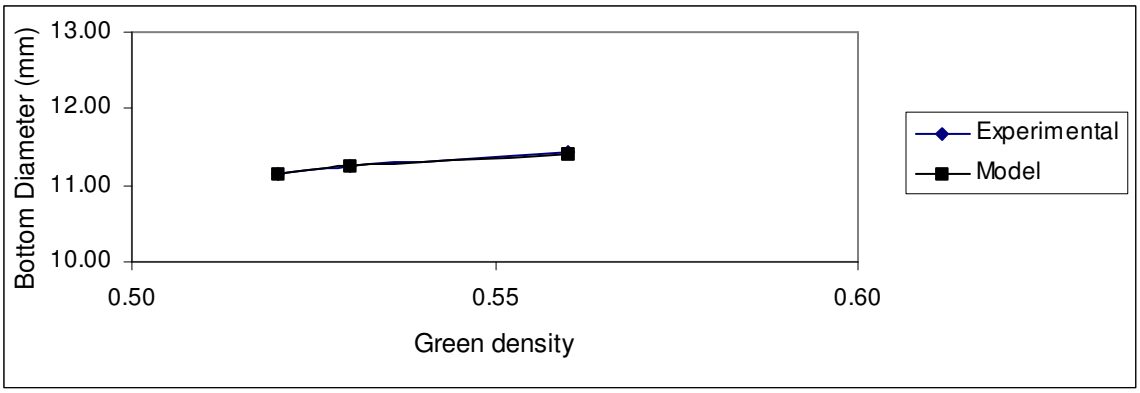

Figure 4 (a)

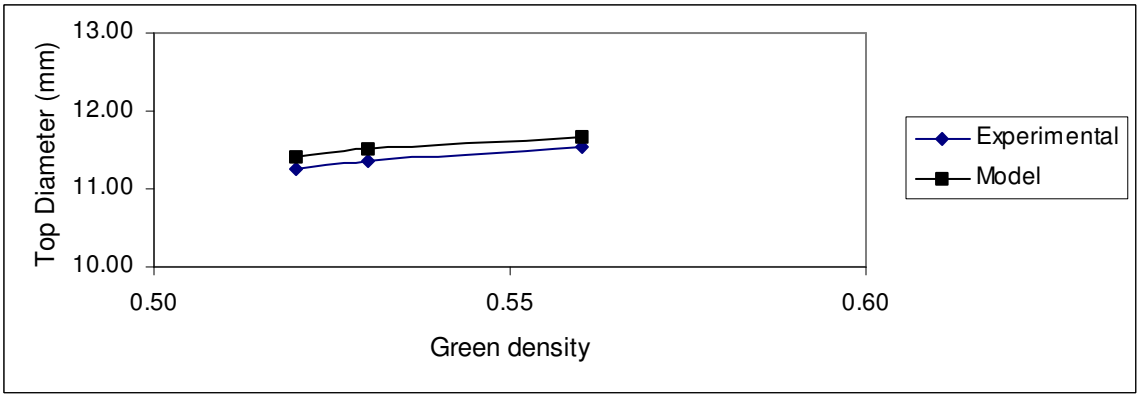

Figure 4 (b)

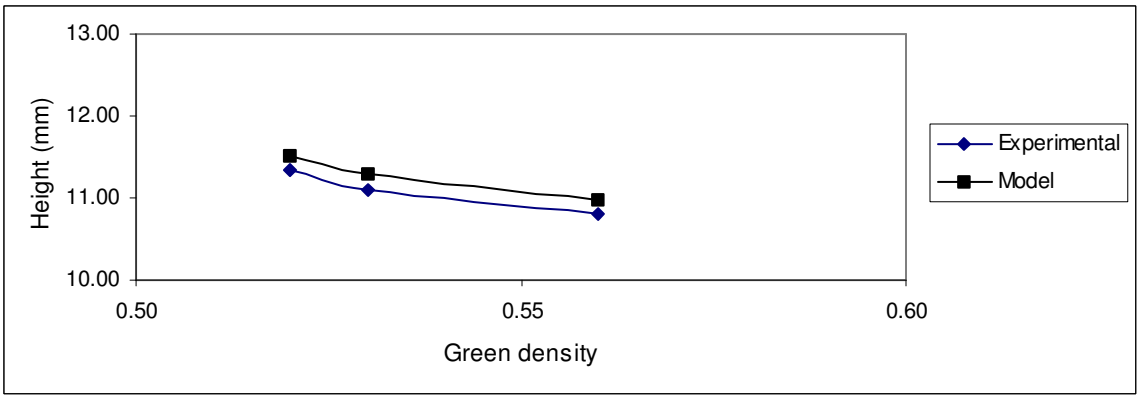

Figure 4 (c)

Figure 4. *Comparison of experimental results with model prediction for grade-2 powder material (a). bottom diameter (b). top diameter (c) .height*

Similarly for the same cylindrical component experiments were conducted with grade-3 powder. The average density of the samples was 0.46, 0.50, 0.54 and 0.57. The shrinkage results of grade-3 powder have similar trend with that of grade-1 and grade-2. Figure-5a, b and c show the comparison of model prediction with experimentally measured dimensions.

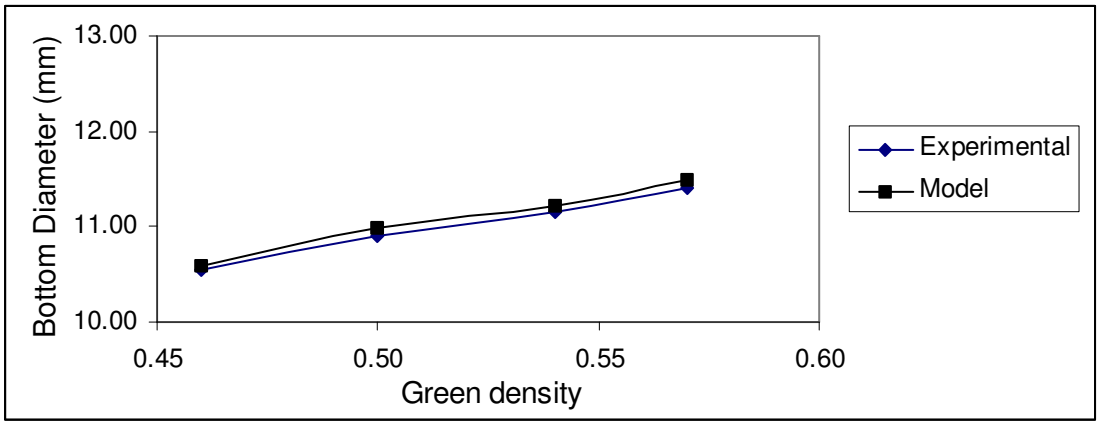

Figure 5 (a)

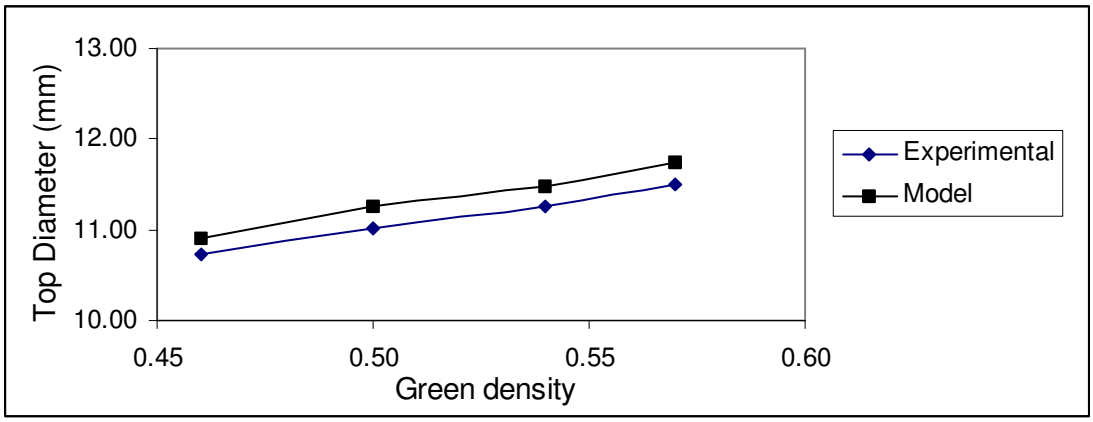

Figure 5 (b)

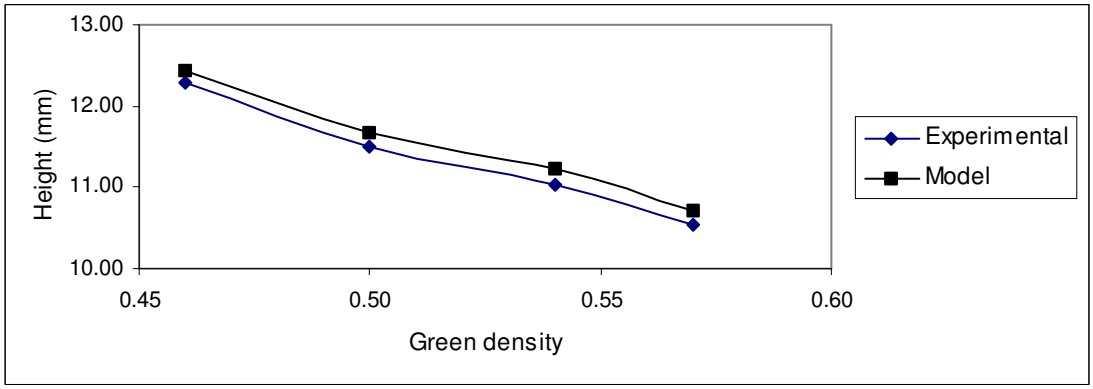

Figure 5 (c)

Figure 5. *Comparison of experimental results with model prediction for grade-3 powder material (a). bottom diameter (b). top diameter (c) .height*

5.2: Component 2

The second component chosen is a tapered cylinder (figure 6a). Top diameter, bottom diameter and height are the three dimensions (figure 6b) considered for validation. Density gradients after compaction are

shown in fig 7a. The component geometry before sintering and after sintering is shown in Figure 7b. The results of validation for grade-1 and grade-2 powder are given in table 1. Compaction procedure for this component is by combined movement of top punch and die. Hence modeling of compaction involves relative movement of die and punch. In this component depending on the grade, which corresponds to different initial powder density, the initial fill volume is different such that the final sintered dimensions are nearly same. This difference in starting volume is considered in the compaction modeling.

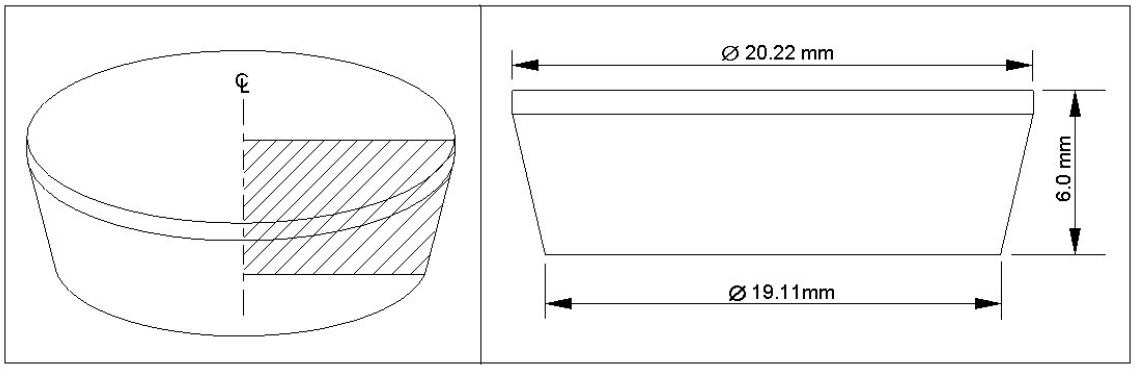

(a) (b)

Figure 6. *(a). Component geometry after compaction (b). Green compact dimensions*

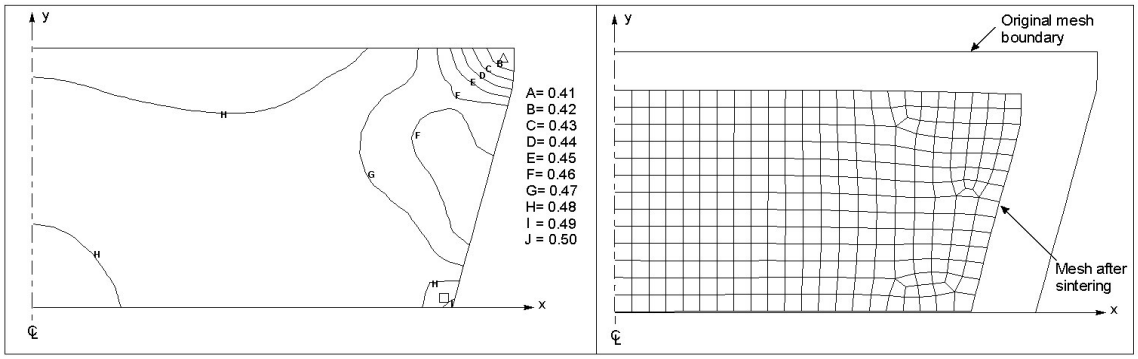

(a) (b)

Figure 7. (a). *Density distribution after compaction (b). Geometry before and after sintering*

Table-1. *Comparison of Sintering experimental results and model prediction for grade-1 powder*

Powder Grade	Bottom Diameter mm		Top Diameter mm		Height mm	
	Experimental	Model	Experimental	Model	Experimental	Model
Grade-1	16.36	16.46	18.59	18.64	5.12	5.30
Grade-2	16.37	16.22	18.49	18.51	5.09	5.16

5: 3: Component 3

The third component is a cylinder with a central through hole as shown in the figure 7. Density gradients at the end of compaction are given in figure 8a. Figure 8b shows prediction of shrinkage after sintering over green compact geometry. Quantitative comparisons are given in table-2. Similar to the taper found in

the first sample, in this case too shrinkage results in taper along the axial direction on the outer surface hence outer diameter is measured on the top side and bottom side. Top outer diameter, bottom outer diameter, inner diameter and height are the four dimensions considered for validation. In this component also the compaction is through combined movement of top punch and die.

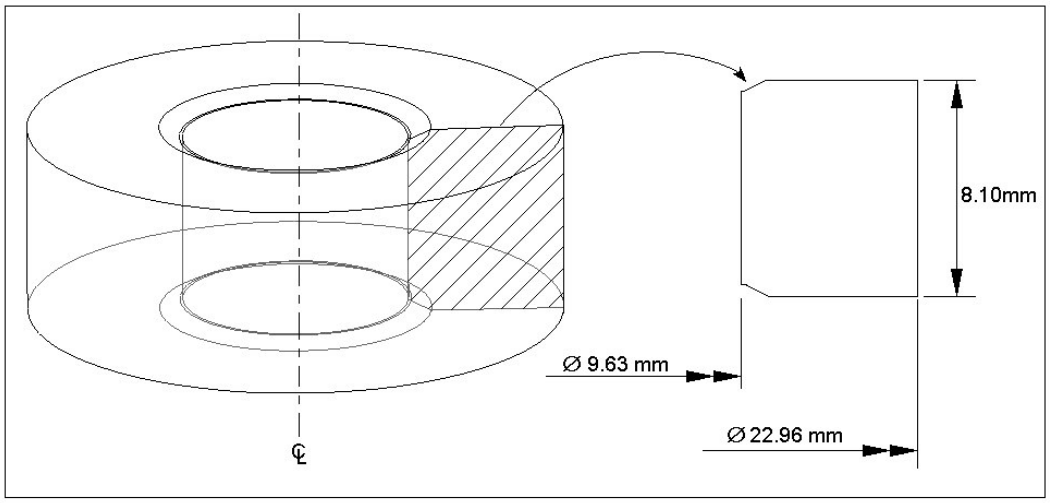

Figure 7. Component geometry *after compaction with green compact dimensions*

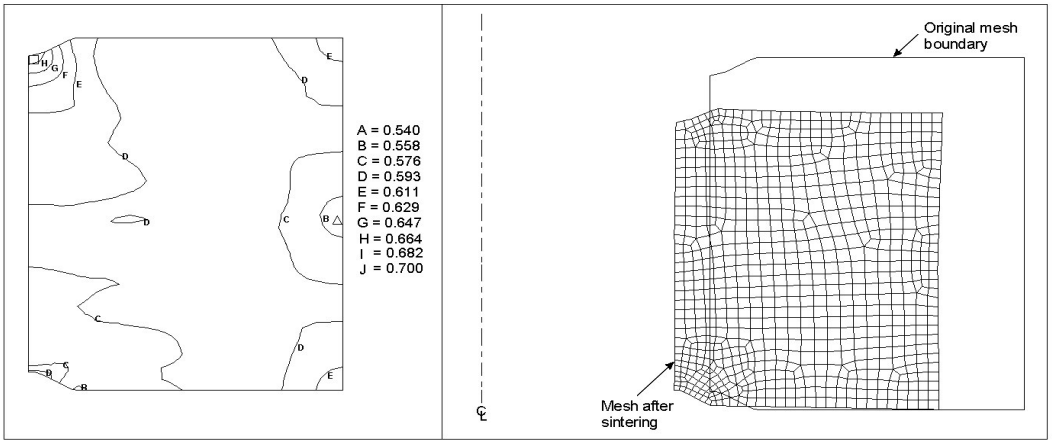

(a) (b)

Figure 8. *(a). Density distribution after compaction (b). Geometry before and after sintering*

Table-2. *Comparison of experimental results and model prediction for grade-1 powder*

Powder grade	ID mm		OD - Bottom mm		OD - Top mm		Height mm	
Grade-1	Exp.	Model	Exp.	Model	Exp.	Model	Exp.	Model
	7.97	8.06	19.04	19.2	19.08	19.36	6.74	6.81

6: DISCUSSION

Comparing the sintering model results with the experimental results, it can be inferred that the sintering model is fairly accurate in modeling the sintering. The model is successful in predicting the final height of

the sintered component with good accuracy and also the taper along the length of the cylinder in the first case. The results for all the three grades of the powder and also for all the sizes of the components considered for simulation are close to the experimentally measured dimensions. The comparison of model predictions with experimental results for the third component is really encouraging as this particular component has a through hole with compound die/punch movement during compaction. In this particular component both inner diameter and outer diameter are shrinking along with height which is captured by the model. Thus it can be concluded that the model is successfully emulating the liquid phase sintering process.

From the validation results it is observed that the sintering model is consistently predicting higher dimension for both top diameter and height for all the samples. This deviation is probably because of the un-accounted wax, which is used as lubricant that flows out of the compact during dewaxing process before the beginning of the sintering process. This wax is of the order of 2-3% of weight. The present model does not account for dewaxing and corresponding reduction in relative density. Further fine-tuning of the model and also a method to incorporate density loss due to wax removal can further improve the accuracy of model predictions.

7: FUTURE SCOPE OF WORK

So far, the insert geometries that can be modeled using 2D axis-symmetric modeling have been considered for validation. The model has to be extended to 3D geometries. Only shrinkage is considered for validation of the model. Though shrinkage is the primary concern for engineer at the industry, other process variables like sintering stress, grain size etc also have significant influence on the soundness of the component produced, hence validation has to be carried for these variables and qualitative and quantitative significance of these variables have to be determined. The final goal of this study is to build a user friendly liquid phase sintering model, which can be deployed at the industry as a product design tool in PM industry.

APENDIX

Table 3. Powder grade composition and Grain size of the constituents

Powder Grade	WC		Co		Cubic Carbides	
	% Composition by weight	Grain size Micron	% Composition by weight	Grain size Micron	% Composition by weight	Grain size Micron
Grade-1	94.0	1.4	6.0	1.6	0.0	-
Grade-2	79.5	1.3	11.5	1.6	9.0	1.5
Grade-3	91.0	2.0	9.0	1.6	0.0	-

REFERENCES

1. G.Petzow and W.A.kaysser "*Basic mechanisms of liquid phase sintering*". Sintered Metal-ceramic composites, 1984

2. J.Svoboda, H.Riedel and Rgeabel, " A m*odel for liquid phase sintering*", Acta metal. Vol.44, 1996, pp3215.
3. P.E. McHugh and H.Riedel, "*A liquid phase sintering model: Application to Si_3N_4 and WC-Co*" Acta metal. v45, 1997, pp2995.
4. S.J.L.Kang, A.Kaysser, G.Petzow, and D.N.Yoon "*Elimination of isolated pores during liquid phase sintering of Mo-Ni*", Powder met., v27[2], 1984, pp97.
5. D.N.Yoon, W.J. Huppmann "*Grain growth and densification during liquid phase sintering of W-Ni*", Acta Metall., v27, 1979, pp693.
6. W.D.KingeryJ, "*Densification during sintering in the presence of liquid phase*". Applied Physics, v30[3], 1959, pp301.
7. S.J.L.Kang, K.H.Kim, and D.N.Yoon J. Am. Ceram. "*Densification and shrinkage during liquid phase sintering*", Soc, v69[2], 1986, pp135.
8. H.H.Park, S.J.Cho, and D.N.Yoon ,"*Pore filling process in Liquid phase sintering*", Metall. Trans.A , v15A, 1984, pp1075.
9. S.M.Lee and S.J.L.Kang ,"*Theoretical analysis of liquid phase sintering: pore filling theory*", Acta Metall., v46, 1998, pp3191.
10. J.Svoboda, H.Riedel, H.Zipse, "*Equilibrium pore surfaces, sintering stresses and constitutive equations for the Intermediate and late stage of sintering-I*.", Acta Metall., v42, 1994, pp435.
11. J.Svoboda, H.Riedel, H.Zipse, "*Equilibrium pore surfaces, sintering stresses and constitutive equations for the Intermediate and late stage of sintering - II*", Acta Metall., v42, 1994, pp445.
12. J. Svoboda, H. Riedel *,"A Theoretical study of grain growth in porous solids during sintering*" Acta Metall., v41, 1993, pp1936.
13. S.Haglund and J.Agren , "*W content in Co binder during sintering of WC-Co*" Acta Metall., v46, 1998, pp2801.
14. O.H.Kown and G.L.Messing *, "Theoretical analysis of solution-precipitation controlled densification during liquid phase sintering"* Acta Metall., v39, 1991, pp2059.
15. Widia India Limited – Experimental data and component, tool geometry drawings.
16. User subroutine manual supplied with DEFORM™ software